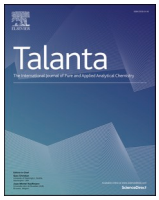
Talanta 266 (2024) 125050



Contents lists available at ScienceDirect

Talanta

journal homepage: www.elsevier.com/locate/talanta





CRISPR-Cas12a-mediated dual-enzyme cascade amplification for sensitive colorimetric detection of HPV-16 target and ATP

Shaohua Gong [a,1], Kexin Song [a,1], Shiqi Zhang [a], Ping Zhou [a], Wei Pan [a], Na Li [a,**], Bo Tang [a,b,*]

[a] College of Chemistry, Chemical Engineering and Materials Science, Key Laboratory of Molecular and Nano Probes, Ministry of Education, Collaborative Innovation Center of Functionalized Probes for Chemical Imaging in Universities of Shandong, Institute of Molecular and Nano Science, Shandong Normal University, Jinan, 250014, PR China

[b] Laoshan Laboratory, Qingdao, 266237, PR China

ARTICLE INFO

Handling Editor: J. Wang

Keywords:
CRISPR-Cas12a
Cascade amplification
HPV-16 DNA
ATP
Colorimetric detection

ABSTRACT

The establishment of sensitive and facile colorimetric platform based on the CRISPR (clustered regularly interspaced short palindromic repeats)-Cas (CRISPR-associated) system is of great significance for in vitro diagnosis. Herein, we develop a dual-enzyme cascade amplification strategy based on CRISPR-Cas12a and glucose oxidase (GOx) for instrument-free and sensitive detection of target analytes. HPV-16 DNA as the model nucleic acid target directly initiated CRISPR-Cas12a-based signal transduction, resulting in the enzymatic cleavage of ssDNA linker and the release of GOx from magnetic nanoparticles 1 (MNPs1). Following simple magnetic separation, the supernatant containing GOx was taken out and used to catalyze the substrate, resulting in a visually detectable color change. The detection limit (LOD) of HPV-16 DNA was as low as 1 pM, and the entire process could be completed within 70 min without the need for expensive equipment. Notably, the dual-enzyme cascade amplification strategy was successfully applied to the detection of non-nucleic acid targets, such as ATP, via a simple signal transduction process. The visual LOD for ATP detection reaches 2.5 μM. The approach provides a robust, sensitive and reliable point-of-care biosensing platform for the detection of target analytes.

1. Introduction

The CRISPR (clustered regularly interspaced short palindromic repeats)-Cas (CRISPR-associated) system is an emerging and promising tool for molecular diagnosis [1–3]. Among the commonly used CRISPR-Cas system for nucleic acid detection, CRISPR-Cas12a is particularly advantageous because of its ability to specifically recognize short DNA sequence of 20 nucleotides and to act as a single-stranded DNase for the degradation of single-stranded DNA (ssDNA) [4–6]. This property of CRISPR-Cas12a reduces the restriction of sequence length and improves the selectivity for nucleic acid detection. Furthermore, the ssDNA cleavage reaction mediated by CRISPR-Cas12a can be performed at a constant temperature of approximately 37 °C, making it suitable for point-of-care testing [7]. However, fluorescence signal is usually adopted as the signal output for target analytes detection, which need to be measured on sophisticated and expensive fluorescence detector [8–10]. Consequently, it is significant to develop instrument-free CRISPR-Cas12a-based methods for point-of-care detection of target analytes.

Colorimetric signal can be directly observed by the naked eye, making them suitable for point-of-care analysis. Currently, gold nanoparticles (AuNPs)-based colorimetric assays and lateral flow strips are usually adopted for endpoint signal detection of CRISPR-Cas12a-mediated amplification reactions [11–13]. Nevertheless, the detection sensitivity is low when CRISPR-Cas12a is employed as the single signal amplifier [14,15]. Although the combination of CRISPR-Cas12a with other exponential amplification methods can improve detection sensitivity, the multistep process increases the operation complexity [16–18]. Therefore, there is a need to further explore a sensitive and easy-to-operate CRISPR-Cas12a-based colorimetric approach for the detection of target analytes.

* Corresponding author. College of Chemistry, Chemical Engineering and Materials Science, Key Laboratory of Molecular and Nano Probes, Ministry of Education, Collaborative Innovation Center of Functionalized Probes for Chemical Imaging in Universities of Shandong, Institute of Molecular and Nano Science, Shandong Normal University, Jinan, 250014, PR China.

** Corresponding author.

E-mail addresses: lina@sdnu.edu.cn (N. Li), tangb@sdnu.edu.cn (B. Tang).

[1] S.G. and K.S. contributed equally to this work.

https://doi.org/10.1016/j.talanta.2023.125050
Received 6 May 2023; Received in revised form 29 July 2023; Accepted 5 August 2023
Available online 7 August 2023
0039-9140/© 2023 Elsevier B.V. All rights reserved.

Herein, we propose a CRISPR-Cas12a-mediated dual-enzyme cascade amplification strategy for facile and sensitive colorimetric detection of target analytes. Human papillomavirus (HPV)-16 DNA was selected as the nucleic acid target, which can directly trigger signal transduction and enable CRISPR-Cas12a to serve as single-stranded DNase to cleave ssDNA. When the ssDNA linker connecting magnetic nanoparticles 1 (MNPs1) and glucose oxidase (GOx) is cleaved, MNPs1 and GOx separate. In the absence of HPV-16 DNA, the MNPs1-GOx remained intact and could be removed by magnetic separation. The presence of HPV-16 DNA induced the CRISPR-Cas12a-mediated enzymatic cleavage reaction, leading to the release of GOx into supernatant from the surface of MNPs1, which then catalyzes the colorless substrate to produce a visible purple color. An additional signal transduction procedure was introduced for ATP detection. Trigger DNA (ATP aptamer) with phosphate backbone was adsorbed on the surface of MNPs2 via the interaction of Fe^{3+} and phosphate backbones of DNA [19–21]. ATP induced desorption of trigger DNA from MNPs2, leading to the activation of CRISPR-Cas12a and the subsequent color change (Scheme 1). The designed approach completely avoids the utilization of expensive equipment for signal detection, and the simple operation yields a visual limit of detection (LOD) for nucleic acid targets as low as 1 pM. The dual-enzyme cascade amplification strategy significantly expands the CRISPR-Cas12a-based colorimetric methodology and offers a promising point-of-care biosensing platform for disease diagnosis.

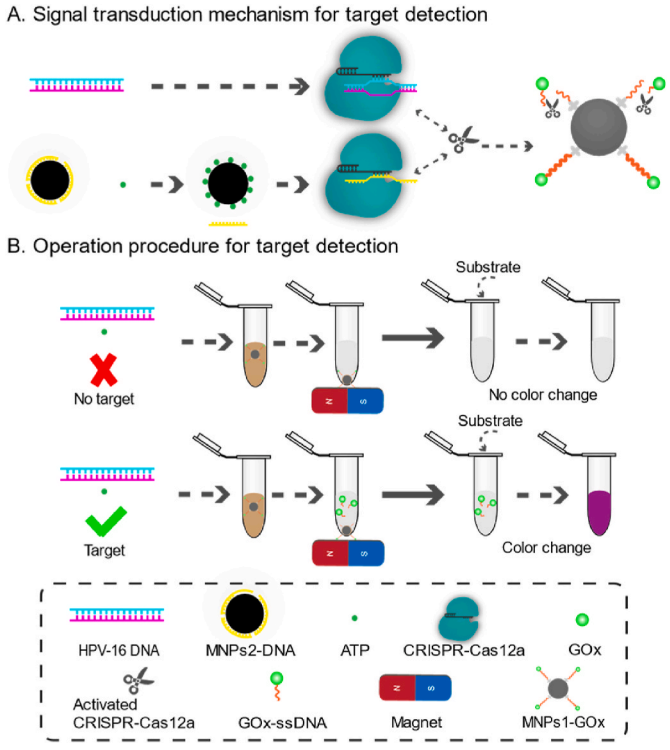
2. Experimental section

2.1. Materials, reagents and instruments

Materials, reagents and instruments are detailed in “Experimental section” in the Supplementary Information (Page S-4).

2.2. Preparation of MNPs1

Ferric chloride anhydrous (0.65 g) and 0.2 g of trisodium citrate were dissolved in 20 mL of ethylene glycol. Afterwards, 1.2 g of sodium acetate was added and the mixture was stirred at room temperature for 30 min. The above solution was introduced into a Teflon-lined stainless-steel autoclave. The sealed autoclave was maintained for 10 h at 200 °C. After that, the black precipitate was collected, washed with ethanol and dried in vacuum.



Scheme 1. CRISPR-Cas12a-mediated dual-enzyme cascade amplification for sensitive colorimetric detection of HPV-16 and ATP.

2.3. Functionalization of vinyl group-terminated ligand on MNPs1

Two hundreds milligram of MNPs1 were washed with MEST (100 mM MES (2-Morpholinoethanesulfonic acid hydrate), pH 5.0, 0.05% tween 20) twice. After that, 200 mg of 1-(3-diaminopropyl)-3-ethylcarbodiimide hydrochloride (EDC) and 200 mg of N-hydroxysuccinimide (NHS) were dissolved in 20 mL of MEST, respectively. The dissolved EDC and NHS were added into 200 mg of MNPs1 and the mixture was shaken at room temperature for 30 min to activate the carboxyl group on MNPs1. The activated MNPs1 was washed with 0.05% tween 20 solution twice. After that, 50 mg of allylamine hydrochloride was dissolved into 20 mL of 0.05% tween 20 solution and the solution was added into the activated MNPs1. The mixture was shaken at room temperature overnight to obtain the vinyl group-terminated ligand functionalized MNPs1 (MNPs1-vinyl). The MNPs1-vinyl was washed with ethanol and then dried in vacuum.

2.4. The preparation of poly(acrylic)acid-coated MNPs1 (MNPs1-PAA)

One hundred milligram of MNPs1-vinyl, 200 mg of MBA, 6 mg of AIBN were dissolved in 80 mL of acetonitrile. Then, 100 μL of MAA was mixed with above solution. The mixture was heated to 115 °C to trigger polymerization reaction. After reflux for 15 min, the distillate was collected. The reaction was stopped after 40 mL of distillate was obtained. The product was collected, washed with water and dried in vacuum.

2.5. Modification of streptavidin on MNPs1-PAA

Ten milligrams of MNPs1-PAA were washed with MEST twice. After that, 10 mg of EDC and 10 mg of NHS were dissolved in 1 mL of MEST, respectively. The dissolved EDC and NHS were added into 10 mg of MNPs1-PAA and the mixture was shaken at room temperature for 30 min to activate the carboxyl group on MNPs1-PAA. The activated MNPs1-PAA was washed with water twice. One hundred microgram of streptavidin was dissolved into 1 mL of water. The streptavidin solution was mixed with the activated MNPs1-PAA overnight to obtain the streptavidin-modified MNPs1 (MNPs1-SA).

2.6. Preparation of ssDNA-modified GOx (GOx-ssDNA)

Preparation of GOx-ssDNA is detailed in "Experimental details" in the Supplementary Information (Page S-5).

2.7. Modification of GOx on MNPs1-SA

The supernatant of 100 μL of MNPs1-SA was removed via magnetic separation. Five microliters of GOx-ssDNA (the used ssDNA here is a biotinylated one) solution were mixed with 95 μL of PBST (PBS, 0.05% tween 20). The above GOx-ssDNA was mixed with MNPs1-SA for 1 h at room temperature. The GOx-functionalized MNPs1 (MNPs1-GOx) was washed with PBST three time and dispersed in 100 μL of PBST for further use.

2.8. Fluorescence recovery experiment

One microliter of CRISPR RNA (crRNA) (1 μM) was first mixed with 1 μL of Cas12a (1 μM). Then, the mixture was added with 15 μL of the reaction buffer D (20 mM Tris-HCl (pH 7.5), 100 mM KCl, 25 mM $MgCl_2$,

0.05% Tween 20) and 2 μL of the ssDNA reporter (10 μM). One microliter of HPV-16 DNA was added into abovementioned solution. The mixture was incubated at 37 °C for 40 min and inactivated at 80 °C for 10 min. After that, 100 μL of water was added and the fluorescence recovery was recorded on a fluorescence spectrometer.

2.9. Preparation of colorimetric substrate

Preparation of colorimetric substrate is detailed in "Experimental details" in the Supplementary Information (Page S-5).

2.10. Native polyacrylamide gel electrophoresis (native-PAGE)

Native-PAGE is detailed in "Experimental details" in the Supplementary Information (Page S-5).

2.11. Preparation of MNPs2-DNA

Preparation of MNPs2 and MNPs2-DNA is detailed in "Experimental details" in the Supplementary Information (Page S-6).

2.12. Detection of ATP in cell lysis buffer

Detection of ATP in cell lysis buffer is detailed in "Experimental details" in the Supplementary Information (Page S-6).

2.13. Detection of HPV-16 DNA in reaction buffer using the developed strategy

The HPV-16 DNA solution (1 μM) was diluted with reaction buffer B (10 mM Tris-HCl, 50 mM NaCl, 20 mM $MgCl_2$, pH 7.9, 0.05% tween 20). One microliter of crRNA (0.375 μM) and 1 μL of Cas12a (0.5 μM) was firstly premixed and then added with 20 μL buffer B and 2 μL of MNPs1-GOx (10 mg/mL). Fifty microliters of HPV-16 DNA solution with different concentrations were added into abovementioned mixture. The resultant mixture was shaken at 37 °C for 1 h. The unreacted MNPs1-GOx was removed via magnetic separation. The supernatant was taken out and added with 180 μL of chromophoric substrate. The mixture was incubated at 37 °C for 10 min to obtain colorimetric signal. Ten microliters of HCl solution (1 M) could be added to stop the colorimetric reaction.

2.14. Detection of HPV-16 DNA in 1% human serum using the developed strategy

The human serum was acquired from hospital. The HPV-16 DNA was spiked into the diluted human serum. The solution was heated at 90 °C for 10 min and the white precipitate was removed via centrifugation to obtain the supernatant. The supernatant was detected via abovementioned procedures.

2.15. Feasibility of the strategy for ATP detection

Fifty microliters of ATP solution were added with 1 μL of trigger DNA absorbed MNPs2 (MNPs-DNA). The mixture was incubated at room temperature for 30 min and then the supernatant was taken out. Cas12a and crRNA was mixed. Then buffer C containing MNPs1-GOx was mixed with CRISPR-Cas12a. The mixture was incubated with the obtained supernatant at 37 °C for 1 h. The unreacted MNPs1-GOx was removed by magnetic separation. The obtained solution was used to react with the substrate for 10 min at 37 °C. Ten microliters of HCl solution (1 M) were used to stop the reaction.

3. Results and discussion

3.1. Synthesis of streptavidin-modified MNPs1

The MNPs1 was synthesized according to previously reported methods [22]. As shown in Fig. 1A, the MNPs1 was successfully prepared and presented spherical shape with rough surface. To improve the dispersity of MNPs1 in solution, the surface of MNPs1 was coated with cross-linked poly(acrylic) acid shell. To achieve the purpose, the surface of MNPs1 was first functionalized with vinyl-terminated ligand to form MNPs1-vinyl. Afterwards, MNPs1-vinyl served as the seeds and the polymerization reaction was initiated to generate poly(acrylic) acid shell on MNPs1 in the presence of N, N′-methylenebisacrylamide (MBA), methacrylic acid (MAA) and 2, 2′-azobisisobutyronitrile (AIBN). The successful preparation of MNPs1-PAA was confirmed by transmission electron microscopy (TEM). As displayed in Fig. 1B, clear shell layer could be found at the edge of the MNPs1 microspheres, suggesting the successful coating of poly(acrylic) acid shell on MNPs1. Besides, the change of zeta potentials was also used to verify the stepwise functionalization of the NPs. Fig. S1 exhibits that the zeta potential of MNPs1 was distinctly negative, which could be attributed to the abundant carboxyl groups on the surface of MNPs1. After modification of vinyl-terminated ligand, the carboxyl groups on MNPs1 were consumed and vinyl groups were labelled, resulting in electric neutrality of MNPs1-vinyl. The coating of poly(acrylic) acid shell introduced the carboxyl groups on MNPs1 again, enabling MNPs1-PAA to be negatively charged. After coated with poly(acrylic) acid shell, the magnetic property of MNPs1 was still retained. MNPs1-PAA could be easily separated via magnet (Fig. S2). Streptavidin was linked to the surface of MNPs1-PAA through amido bond. After functionalization of streptavidin, MNPs1-PAA could be utilized to combine biotinylated DNA. As shown in Fig. S3, no DNA band was observed in lane b after the biotinylated DNA reacted with MNPs1-SA, which suggested the successful modification of SA on MNPs1. To investigate the combination ability of MNPs1-SA for biotinylated DNA, the signals of different concentrations of DNA measured on NanoDrop One were used to establish the calibration curve. The binding capacity of MNPs1-SA for biotinylated DNA was calculated to be 0.19 nmol/mg based on the calibration curve in Fig. S4.

3.2. Preparation for GOx-modified MNPs1

To immobilize GOx on MNPs1-PAA, GOx was first functionalized with maleimide group to react with thiolated ssDNA, forming GOx-ssDNA conjugate. As shown in Fig. S5, the thiolated ssDNA freely migrated in lane a. However, the migration of ssDNA was completely impeded in lane b, demonstrating ssDNA was successfully attached on GOx. The prepared GOx-ssDNA conjugate was further linked to MNPs1-SA through biotin-streptavidin affinity to obtain GOx-modified MNPs1 (MNPs1-GOx). Fig. S6 shows that the MNPs1-SA incubated with GOx-ssDNA could efficiently react with substrate to generate visual purple color. The colorimetric reaction of GOx has been illustrated with chemical equations (Fig. S7). The GOx lacked of ssDNA could not be modified on MNPs1-SA due to the absence of biotin, causing the colorless of solution. The results demonstrated that GOx was immobilized on MNPs1-SA with ssDNA and the formed MNPs1-GOx could be utilized for following experiments.

3.3. Feasibility of the developed strategy

The feasibility of the CRISPR-Cas12a-based dual-enzyme cascade amplification strategy was investigated. The single-stranded DNase property of CRISPR-Cas12a was confirmed by native polyacrylamide gel electrophoresis (PAGE) and fluorescence assay. As shown in Fig. 1C, the intensity of crRNA band weakened in lane b compared with that in lane a, suggesting the combination of Cas12a and crRNA. In the absence of

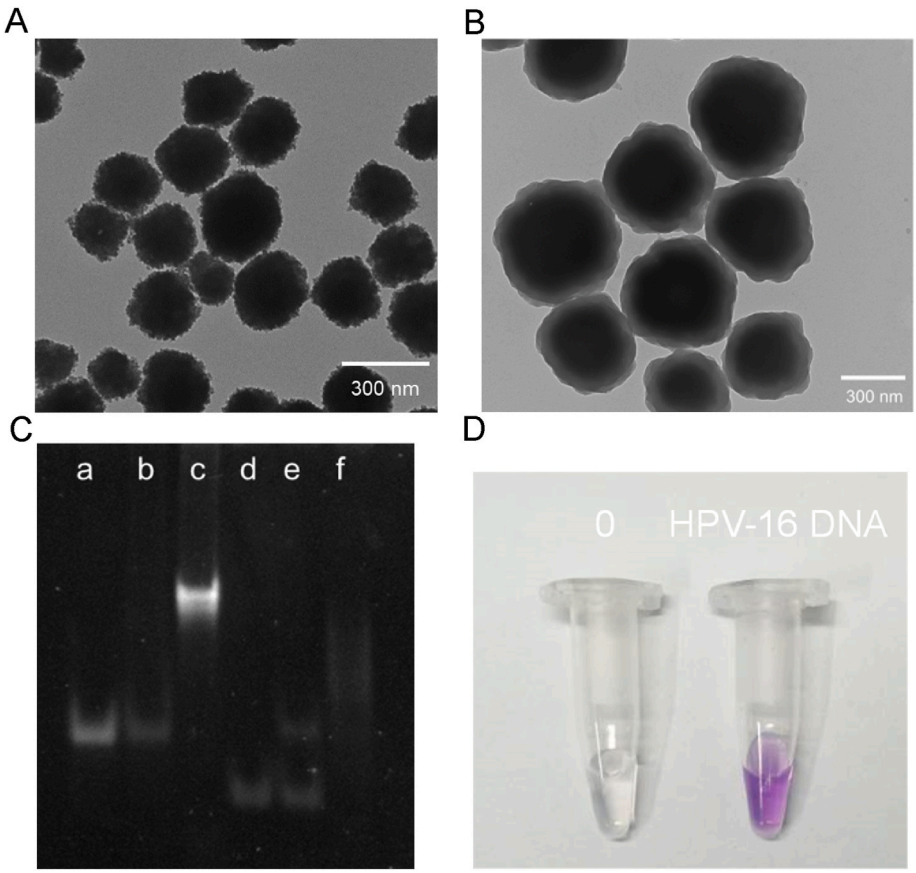


Fig. 1. (A) The TEM image of MNPs1. (B) The TME image of MNPs1-PAA. (C) Native-PAGE image of activated CRISPR-Cas12a for ssDNA cleavage. (a) crRNA; (b) crRNA + Cas12a; (c) HPV-16 DNA; (d) ssDNA; (e) ssDNA + crRNA + Cas12a; (f) HPV-16 DNA + CRISPR-Cas12a + ssDNA. (D) Color change after HPV-16 DNA was added and detected with the developed strategy.

HPV-16 DNA, the collateral cleavage property was not initiated and the band intensity of ssDNA substrate in lane e was not changed compared with that in lane d. By contrast, only dispersive DNA band was remained in lane f, which could be regarded as the cleaved ssDNA by activated CRISPR-Cas12a. The results suggested that the addition of HPV-16 DNA could successfully activate CRISPR-Cas12a to cut ssDNA substrate. The activation of CRISPR-Cas12a was also verified by fluorescence assay. As shown in Fig. S8, the fluorescence intensity was only enhanced when HPV-16 DNA was introduced into the reaction system, demonstrating the successful activation of CRISPR-Cas12a for degradation of ssDNA reporter. Afterwards, the cleavage activity of CRISPR-Cas12a for ssDNA linker on MNPs1 was studied. Once breakage of ssDNA linker, GOx was released into supernatant and could be used to further catalyze substrate to generate color change. Fig. 1D displays that the solution successfully turned into purple color after added with HPV-16 DNA, confirming the feasibility of the developed strategy for colorimetric detection of target nucleic acid.

3.4. Optimization of the reaction conditions

Next, the parameters that influence the detection performance, including the ratio of Cas12a and crRNA, reaction buffer, concentration of magnesium ion (Mg^{2+}) and incubation time, were optimized. As displayed in Fig. S9 and Fig. 2A, the lack of crRNA leaded to almost no color change, demonstrating the importance of crRNA for the cleavage activity of CRISPR-Cas12a. With addition of crRNA, obvious purple color appeared. The optimized ratio of Cas12a and crRNA was determined to be 1:0.75. Next, different reaction buffers were tested and selected for cleavage reaction. Fig. S10 and Fig. 2B shows that the buffer A (10 mM Tris-HCl (pH 7.9), 10 mM $MgCl_2$, 50 mM NaCl) exhibited better performance compared with buffer C (20 mM Tris-HCl (pH 7.5), 25 mM $MgCl_2$, 100 mM KCl). Notably, the buffer B (10 mM Tris-HCl (pH 7.9), 10 mM $MgCl_2$, 50 mM NaCl, 0.05% tween 20) and buffer D (20 mM Tris-HCl (pH 7.5), 25 mM $MgCl_2$, 100 mM KCl, 0.05% tween 20), which were added with 0.05% tween20, presented deeper color change compared with buffer A and buffer C. This could be attributed to that tween 20 was a non-ionic surfactant and could eliminate the electrostatic interaction between MNPs1, ssDNA and GOx, thereby minimizing the steric hindrance for CRISPR-Cas12a cleavage. Hence, buffer B was chosen as the reaction buffer. Mg^{2+} was another significant parameter for CRISPR-Cas12a cleavage and thus its concentration was optimized. As can be seen in Fig. S11 and Fig. 2C, almost no color could be seen in the absence of Mg^{2+}. With the concentration of Mg^{2+} increasing, the color of solution gradually became obvious. 20 mM of Mg^{2+} was enough to produce distinct color change and thus the concentration was selected for further use. The incubation time of activated CRISPR-Cas12a with MNPs1-GOx was studied. Fig. S12 and Fig. 2D presents that the color changes of solution gradually increased with the extension of incubation time. When the incubation time exceeded 60 min, the color of solution was not significantly changed. Therefore, 60 min was used as the optimized incubation time for subsequent experiments.

3.5. Detection performance of the developed strategy

The detection performance was explored using the optimized reaction conditions. As exhibited in Fig. 3A, the purple color gradually became clear with the increase of HPV-16 DNA concentration. To study the change of colorimetric signal with the concentration of HPV-16 DNA, the absorbance of solution at 556 nm was recorded. The correlation equation was $Y = 0.33892lgX+0.01249$ (Pearson's $r = 0.98917$) in

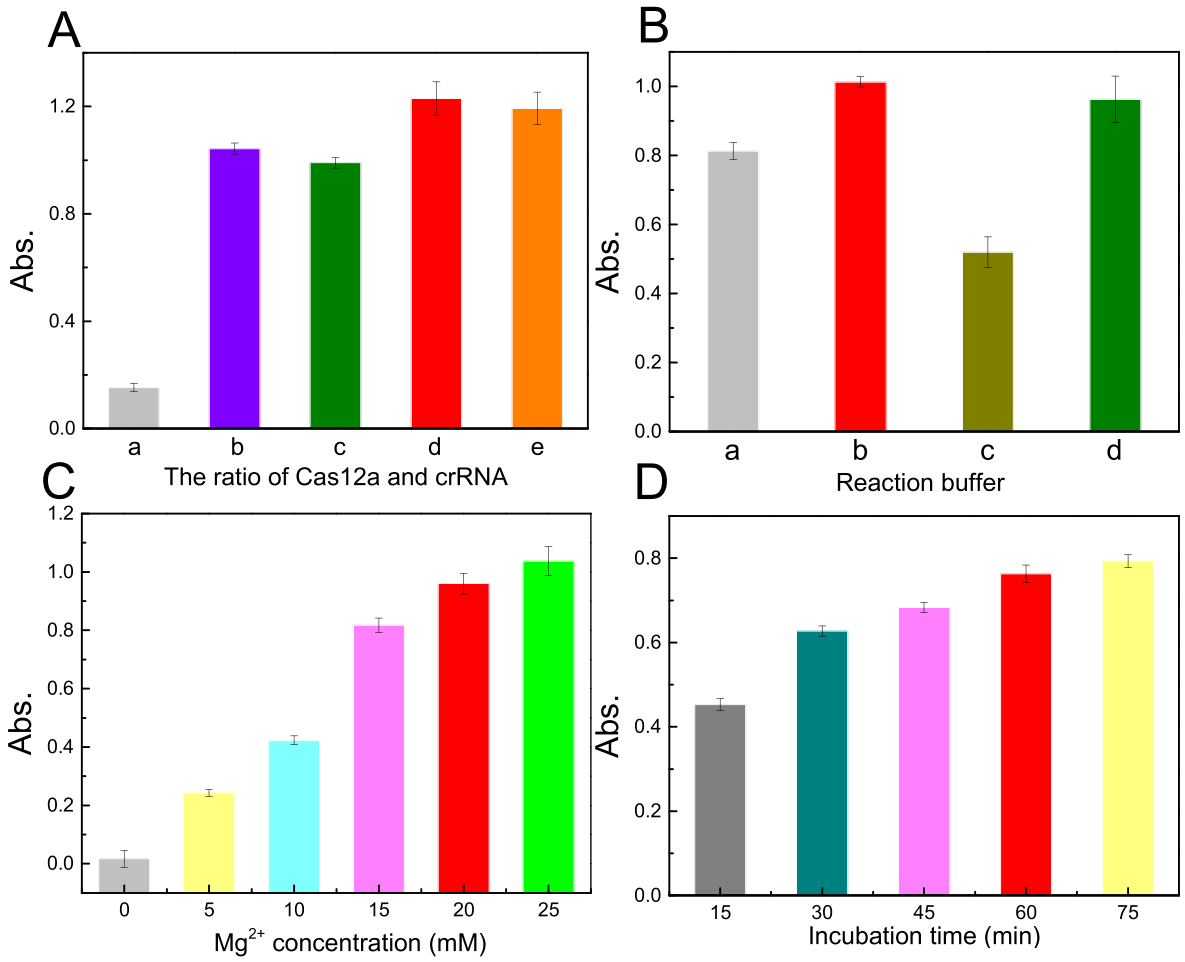


Fig. 2. (A) The UV–vis absorbance of solution using different ratio of Cas12a and crRNA for HPV-16 DNA detection. (a) 1:0; (b) 1:0.25; (c) 1:0.5; (d) 1:0.75; (e) 1:1. (B) UV–vis absorbance of solution using different reaction buffer for HPV-16 DNA detection. (a) buffer A (10 mM Tris-HCl (pH 7.9), 10 mM $MgCl_2$, 50 mM NaCl); (b) buffer B (10 mM Tris-HCl (pH 7.9), 10 mM $MgCl_2$, 50 mM NaCl, 0.05% tween 20). (c) buffer C (20 mM Tris-HCl (pH 7.5), 25 mM $MgCl_2$, 100 mM KCl); (d) buffer D (20 mM Tris-HCl (pH 7.5), 25 mM $MgCl_2$, 100 mM KCl, 0.05% tween 20). (C) The UV–vis absorbance of solution using different concentrations of Mg^{2+} for HPV-16 DNA detection. (D) The UV–vis absorbance of solution using different incubation times for HPV-16 DNA detection.

the range of 1 pM to 1 nM (Fig. 3B, Fig. S13). For colorimetric detection, it is also crucial to explore the lowest concentration of target DNA that could generate distinguishable color change. As shown in Fig. S14, the colorimetric signal produced by 1 pM of HPV-16 DNA could be distinguished by naked eye. And the color contrast became more obvious when the concentration of target DNA reached 5 pM. The reproductivity of the developed strategy was also tested. As shown in Fig. S15, in the absence of HPV-16 DNA, the solutions presented colorless. By contrast, in the presence of 100 pM of HPV-16 DNA, distinct purple color appeared in the solutions and the results of five parallel measurements displayed no obvious difference. The relative standard deviation (RSD) was calculated to be 2.70%. The results suggested that the reproductivity of the developed strategy was satisfactory. The strategy was compared with other previously reported method for HPV-16 DNA detection. As shown in Table S1, the strategy did not require specific instruments and could detect HPV-16 DNA with satisfactory sensitivity in a short time..

Next, the detection selectivity of the developed strategy was investigated using HPV-18 as the interfering DNA. As exhibited in Fig. 4A and B, no color change was found in control group (group a). And as same as the result in group a, 1 nM of interfering HPV-18 DNA in group c was also not able to generate visible colorimetric signal. In comparison, 100 pM of HPV-16 DNA in group b produced remarkable purple color, demonstrating the specific recognition of CRISPR-Cas12a for HPV-16 DNA. Notably, when 100 pM of HPV-16 was mixed with 1 nM of HPV-18 (group d), the generated colorimetric signal was comparable to that in group b. The result suggested that the presence of interfering DNA would not affect the cleavage of CRISPR-Cas12a for ssDNA linkers on MNPs1 and the generation of colorimetric signal.

It has been reported that HPV-16 DNA could also be found in the serum of cervical cancer patients [23,24]. To examine the anti-interference capacity and detection accuracy of the developed strategy, the HPV-16 DNA was spiked in 1% human serum for detection. As shown in Fig. 5, the UV–vis absorbance of solution increased with the increasing concentration of spiked HPV-16 DNA. Notably, the UV–vis absorbance of solution in 1% human serum at different concentrations of HPV-16 DNA were almost consistent with that in reaction buffer, which demonstrated that the good anti-interference ability of the developed strategy for HPV-16 DNA detection in the presence of other interfering substances. The storage stability of reagents was an important factor for real application and thus was examined. As displayed in Fig. S16, the color of substrate has no significant change after storage at 4 °C and at room temperature for 1 month. When added with GOx, the substrate could be catalyzed and generate color change. The above result demonstrated that the developed strategy possessed potential practicability for real application in resource-restrained areas.

3.6. Adenosine triphosphate detection using the developed strategy

The dual-enzyme cascade amplification strategy was also applied to

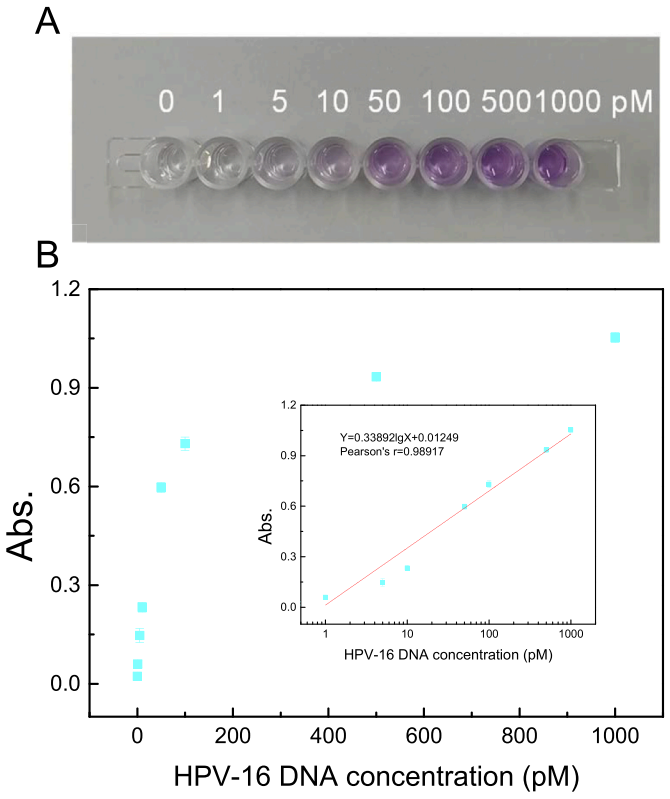


Fig. 3. (A) Colorimetric signal change of solution with the increasing concentrations of HPV-16 DNA. (B) The UV–vis absorbance of solution in (A).

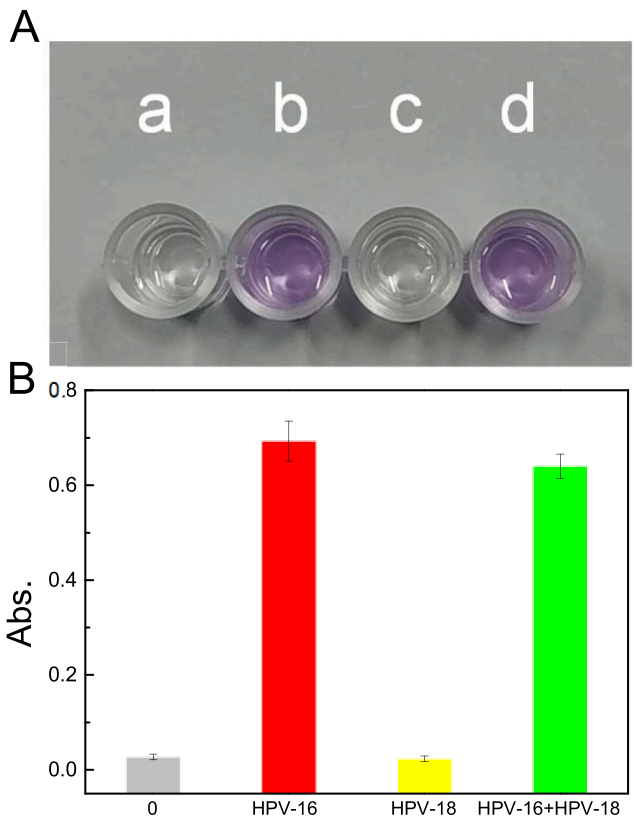


Fig. 4. (A) (a) 0; (b) HPV-16 DNA (100 pM); (c) HPV-18 DNA (1 nM); (d) HPV-16 DNA (100 pM) + HPV-18 DNA (1 nM). (B) The UV–vis absorbance of solution in (A).

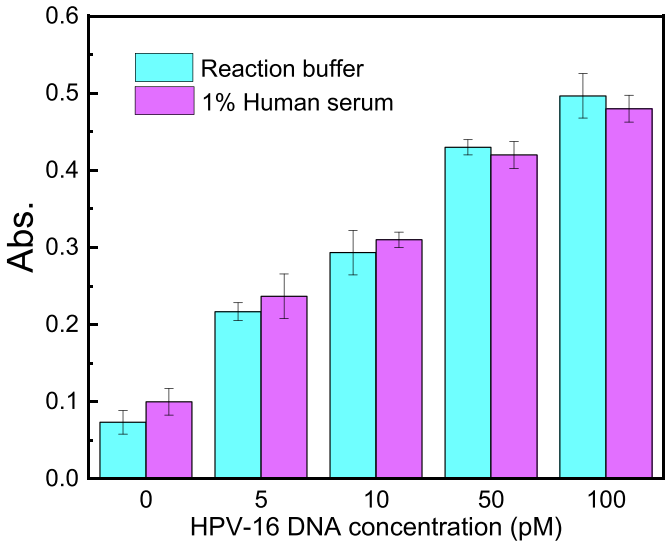


Fig. 5. UV–vis absorbance of solution triggered by different concentrations of HPV-16 DNA in buffer and 1% human serum.

the detection of non-nucleic acid target. Adenosine triphosphate (ATP) was chosen as the model target. To realize the signal transduction of ATP, trigger DNA-absorbed magnetic nanoparticles 2 (MNPs2-DNA) were synthesized. The incubation of ATP and MNPs2-DNA could release the trigger DNA from MNPs2, which activated the *trans*-cleavage activity of CRISPR-Cas12a and initiated the cascade amplification for colorimetric detection. The successful preparation of MNPs2-DNA was first characterized. As shown in Fig. S17, the spherical MNPs2 with a diameter of approximate 300 nm were obtained. The conjugation of trigger DNA with MNPs2 was also verified. Fig. S18 shows that the DNA concentration in supernatant was significantly decreased after DNA was treated with MNPs2, and the washing procedure would not release DNA from MNPs2, demonstrating that the successful absorption of DNA on MNPs2. The feasibility of the developed strategy for ATP detection was investigated. ATP was first incubated with MNPs2-DNA. Then the unreacted MNPs2-DNA were removed via magnetic separation and the supernatant was detected by the cascade amplification strategy. As can be seen in Fig. S19, the solution remains colorless in the absence of ATP. In comparison, the addition of ATP leaded to obvious color change in solution. The results suggested that the cascade amplification strategy could be successfully be used for ATP detection.

Next, different concentrations of ATP was detected by the dual-enzyme cascade amplification strategy. As shown in Fig. 6A, the solution color deepened with increasing concentration of ATP. Fig. 6B and Fig. S20 shows that the absorbance of solution was linearly related to the ATP concentration in the range of 0–50 μM (Y = 0.01952X+0.09009, Pearson's r = 0.99413), and nearly reached a plateau when the concentration of ATP was 100 μM. And the visual LOD was determined to be 2.5 μM via naked eyes (Fig. S21). The detection sensitivity was comparable to many previously reported colorimetric methods for ATP detection (Table S2).

The detection specificity of the dual-enzyme cascade amplification strategy for ATP was studied. Metal ions (Na^+, Zn^{2+}, Ca^{2+}, Cu^{2+}, Mg^{2+}), anions (NO_3^-, CO_3^{2-}) and nucleotides (GTP, CTP, UTP) were chosen as the interfering substances. As shown in Fig. 7 and Fig. S22, only ATP could induce obvious color change, demonstrating that the developed strategy could selectively detect ATP.

The practicability of the dual-enzyme cascade amplification strategy in more complex media was studied. It has been reported that ATP was aberrantly expressed in cancer cells [25,26].Thus, ATP in cell lysis

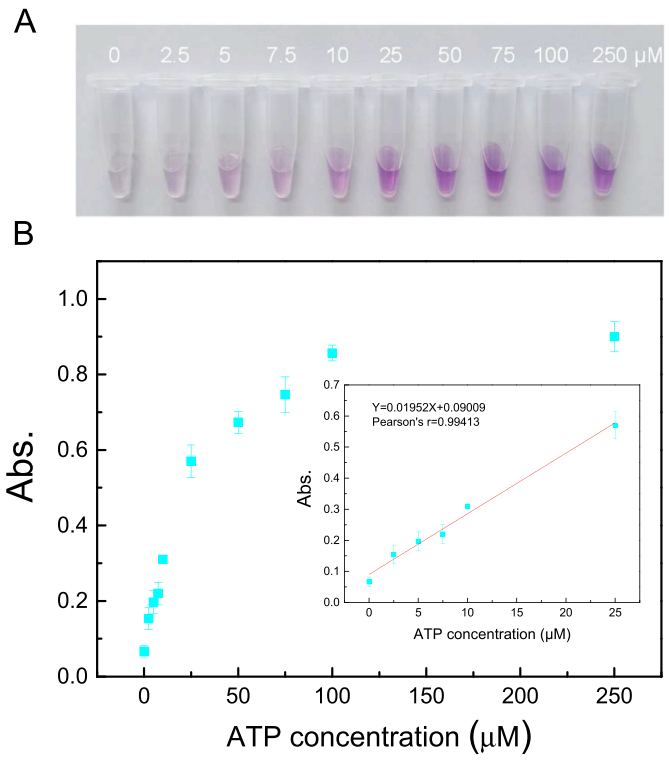


Fig. 6. (A) Colorimetric signal change of solution with the increasing concentration of ATP. (B) UV–vis absorbance of solution with the increasing concentration of ATP.

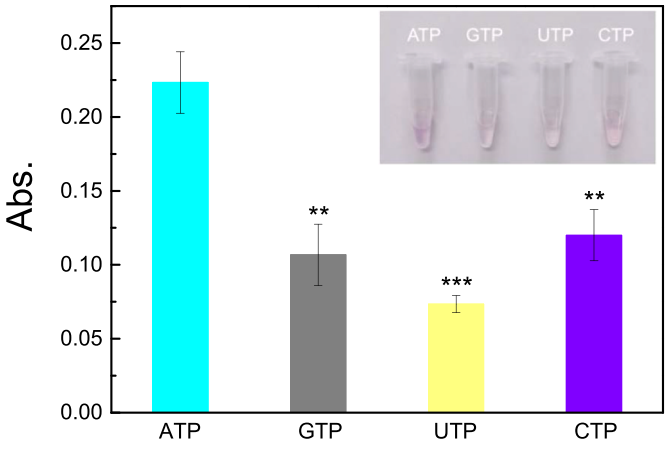


Fig. 7. Detection specificity of the developed strategy for ATP and its analogues. P values were calculated using the Student's t-test (***P < 0.001, and **P < 0.01) to compare other groups with experimental group.

buffer was detected by the developed strategy. Fig. 8 shows that more obvious color change could be seen along with the increasing cell numbers, suggesting that the strategy could be successfully used for ATP detection in real samples.

4. Conclusion

In summary, we have developed a facile and sensitive colorimetric biosensing strategy based on dual-enzyme mediated cascade signal amplification. For nucleic acid target detection, the HPV-16 DNA could successfully initiate the enzyme mediated cascade signal amplification, leading to the generation of visual color change in 70 min. Our method demonstrated excellent detection sensitivity, selectivity and anti-

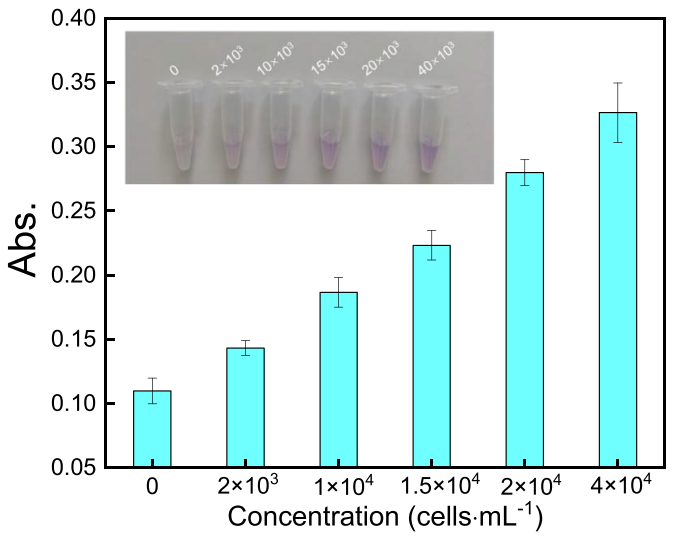


Fig. 8. UV–vis absorbance and colorimetric signal change of solution when ATP in cell lysis buffer was detected.

interference capability for nucleic acid target detection, as well as the detection of non-nucleic acid target ATP. The visual limit of detection (LOD) for HPV-16 DNA was as low as 1 pM, and the colorimetric signal generated by the target analytes could be easily distinguished with the naked eye. Our approach completely avoids the use of costly equipment for signal detection and provides a potential point-of-care biosensing platform for disease diagnosis. This dual-enzyme cascade amplification strategy expands the CRISPR-Cas12a-based colorimetric methodology and has great potential for various biosensing applications.

CRediT authorship contribution statement

Shaohua Gong: Conceptualization, Data curation, Methodology, Writing – original draft. **Kexin Song:** Methodology, Data curation, Validation. **Shiqi Zhang:** Data curation, Formal analysis. **Ping Zhou:** Resources. **Wei Pan:** Writing – review & editing. **Na Li:** Project administration, Funding acquisition, Supervision, Writing – review & editing. **Bo Tang:** Project administration, Funding acquisition, Supervision, Writing – review & editing.

Declaration of competing interest

The authors declare that they have no known competing financial interests or personal relationships that could have appeared to influence the work reported in this paper.

Data availability

Data will be made available on request.

Acknowledgment

Shandong Provincial Key Research and Development Program (Major Scientific and Technological Innovation Project) ; Local Science and Technology Development Fund Guided by the Central Government of Shandong Province ; Youth Innovation Science and Technology Program of Higher Education Institution of Shandong Province; Jinan Innovation Team.

Appendix A. Supplementary data

Supplementary data to this article can be found online at https://doi.org/10.1016/j.talanta.2023.125050.

References

[1] M.M. Kaminski, O.O. Abudayyeh, J.S. Gootenberg, F. Zhang, J.J. Collins, CRISPR-based diagnostics, Nat. Biomed. Eng. 5 (2021) 643–656.

[2] W. Feng, A.M. Newbigging, J. Tao, Y. Cao, H. Peng, C. Le, J. Wu, B. Pang, J. Li, D. L. Tyrrell, H. Zhang, X.C. Le, CRISPR technology incorporating amplification strategies: molecular assays for nucleic acids, proteins, and small molecules, Chem. Sci. 12 (2021) 4683–4698.

[3] S. Gong, S. Zhang, F. Lu, W. Pan, N. Li, B. Tang, CRISPR/Cas-Based in vitro diagnostic platforms for cancer biomarker detection, Anal. Chem. 93 (2021) 11899–11909.

[4] J.S. Chen, E. Ma, L.B. Harrington, M.D. Costa, X. Tian, J.M. Palefsky, J.A. Doudna, CRISPR-Cas12a target binding unleashes indiscriminate single-stranded DNase activity, Science 360 (2018) 436–439.

[5] S. Gong, J. Li, W. Pan, N. Li, B. Tang, Duplex-specific nuclease-assisted CRISPR-Cas12a strategy for MicroRNA detection using a personal glucose meter, Anal. Chem. 93 (2021) 10719–10726.

[6] S. Gong, S. Zhang, X. Wang, J. Li, W. Pan, N. Li, B. Tang, Strand displacement amplification assisted CRISPR-Cas12a strategy for colorimetric analysis of viral nucleic acid, Anal. Chem. 93 (2021) 15216–15223.

[7] J.S. Gootenberg, O.O. Abudayyeh, M.J. Kellner, J. Joung, J.J. Collins, F. Zhang, Multiplexed and portable nucleic acid detection platform with Cas13,Cas12a, and Csm6, Science 360 (2018) 439–444.

[8] L. Peng, J. Zhou, G. Liu, L. Yin, S. Ren, S. Man, L. Ma, CRISPR-Cas12a based aptasensor for sensitive and selective ATP detection, Sensor. Actuator. B Chem. 320 (2020), 128164.

[9] S. Peng, Z. Tan, S. Chen, C. Lei, Z. Nie, Integrating CRISPR-Cas12a with a DNA circuit as a generic sensing platform for amplified detection of microRNA, Chem. Sci. 11 (2020) 7362–7368.

[10] W. Tian, X. Liu, G. Wang, C. Liu, A hyperbranched transcription-activated CRISPR-Cas12a signal amplification strategy for sensitive microRNA sensing, Chem. Commun. 56 (2020) 13445–13448.

[11] L. Ma, L. Peng, L. Yin, G. Liu, S. Man, CRISPR-Cas12a-Powered dual-mode biosensor for ultrasensitive and cross-validating detection of pathogenic bacteria, ACS Sens. 6 (2021) 2920–2927.

[12] Y. Li, H. Mansour, T. Wang, S. Poojari, F. Li, Naked-eye detection of grapevine red-blotch viral infection using a plasmonic CRISPR Cas12a assay, Anal. Chem. 91 (2019) 11510–11513.

[13] M. Chen, R. Luo, S. Li, H. Li, Y. Qin, D. Zhou, H. Liu, X. Gong, J. Chang, Paper-based strip for ultrasensitive detection of OSCC-associated salivary MicroRNA via CRISPR/Cas12a Coupling with IS-primer amplification reaction, Anal. Chem. 92 (2020) 13336–13342.

[14] M. Bao, E. Jensen, Y. Chang, G. Korensky, K. Du, Magnetic bead-quantum dot (MB-Qdot) clustered regularly interspaced short palindromic repeat assay for simple viral DNA detection, ACS Appl. Mater. Interfaces 12 (2020) 43435–43443.

[15] J.H. Choi, J. Lim, M. Shin, S.H. Paek, J.W. Choi, CRISPR-Cas12a-Based nucleic acid amplification-free DNA biosensor via Au nanoparticle-assisted metal-enhanced fluorescence and colorimetric analysis, Nano Lett. 21 (2021) 693–699.

[16] Y. Jiang, M. Hu, A.A. Liu, Y. Lin, L. Liu, B. Yu, X. Zhou, D.W. Pang, Detection of SARS-CoV-2 by CRISPR/Cas12a-Enhanced Colorimetry, ACS Sens. 6 (2021) 1086–1093.

[17] C. Yuan, T. Tian, J. Sun, M. Hu, X. Wang, E. Xiong, M. Cheng, Y. Bao, W. Lin, J. Jiang, C. Yang, Q. Chen, H. Zhang, H. Wang, X. Wang, X. Deng, X. Liao, Y. Liu, Z. Wang, G. Zhang, X. Zhou, Universal and naked-eye gene detection platform based on the clustered regularly interspaced short palindromic repeats/Cas12a/13a system, Anal. Chem. 92 (2020) 4029–4037.

[18] W.S. Zhang, J. Pan, F. Li, M. Zhu, M. Xu, H. Zhu, Y. Yu, G. Su, Reverse transcription recombinase polymerase amplification Coupled with CRISPR-Cas12a for facile and highly sensitive colorimetric SARS-CoV-2 detection, Anal. Chem. 93 (2021) 4126–4133.

[19] B. Liu, J. Liu, DNA adsorption by magnetic iron oxide nanoparticles and its application for arsenate detection, Chem. Commun. 50 (2014) 8568–8570.

[20] S. Li, X. Zhao, X. Yu, Y. Wan, M. Yin, W. Zhang, B. Cao, H. Wang, Fe_3O_4 nanozymes with aptamer-tuned Catalysis for selective colorimetric analysis of ATP in blood, Anal. Chem. 91 (2019) 14737–14742.

[21] A. Lopez, J. Liu, Nanomaterial and aptamer-based sensing: target binding versus target adsorption illustrated by the detection of adenosine and ATP on metal oxides and graphene oxide, Anal. Chem. 93 (2021) 3018–3025.

[22] S. Gong, Y. Chen, W. Pan, N. Li, B. Tang, An in vitro site-specific cleavage assay of CRISPR-Cas9 using a personal glucose meter, Chem. Commun. 56 (2020) 8850–8853.

[23] C.M. Ho, S.S. Yang, T.Y. Chien, S.H. Huang, C.J. Jeng, S.F. Chang, Detection and quantitation of human papillomavirus type 16, 18 and 52 DNA in the peripheral blood of cervical cancer patients, Gynecol. Oncol. 99 (2005) 615–621.

[24] J.H. Tsou, Q. Leng, F. Jiang, A CRISPR test for detection of Circulating nuclei acids, Transl. Oncol. 12 (2019) 1566–1573.

[25] D. Song, H. Li, H. Wang, Y. Tang, Y. Feng, B. Li, Dual-hairpin ligation amplification enabled ultra-sensitive and selective ATP detection for cancer monitor, Biosens. Bioelectron. 212 (2022), 114402.

[26] F. Wu, W. Liu, S. Yang, Q. Yao, Y. Chen, X. Weng, X. Zhou, An aptamer-based ligation-triggered rolling circle amplification strategy for ATP detection and imaging in situ, J. Photochem. Photobiol., A 355 (2018) 114–119.